micromod Partikeltechnologie GmbH

modular designed particles

Publications and Reviews

Technological Applications

Implementation in Life Sciences

magnetic micro- and nanoparticles

www.micromod.de

Product overview

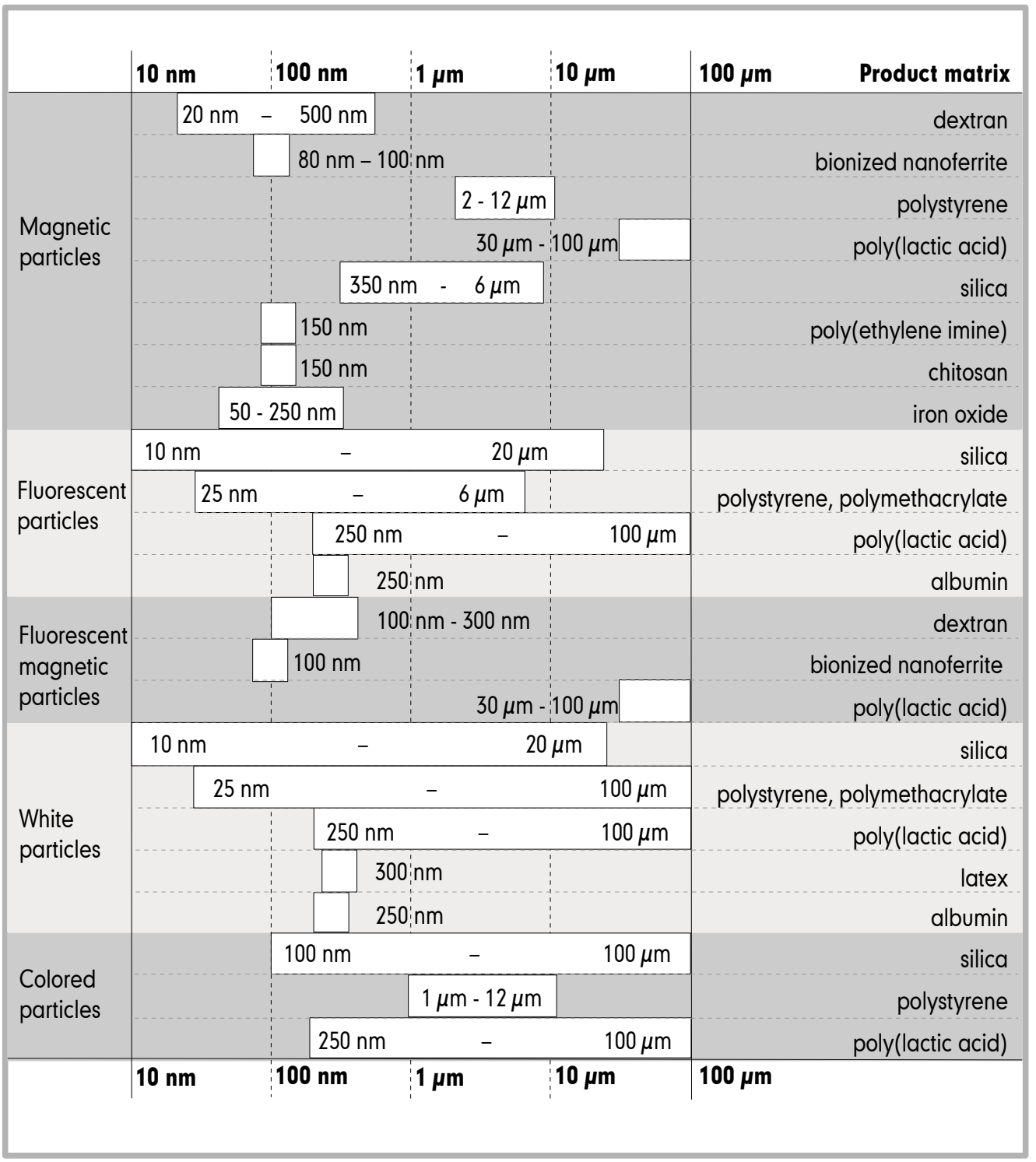

micromod Partikeltechnologie GmbH
Friedrich-Barnewitz-Straße 4, D-18119 Rostock
Tel.:+49 381/54 34 56 10, Fax: +49 381/54 34 56 20
Technical Support Tel.: +49 381/54 34 56 14
E-mail: info@micromod.de, Internet: www.micromod.de

6 Magnetic nanoparticles for hyperthermia applications

Kerstin Witte[1], Cordula Grüttner[2]

[1] *University of Rostock, Institute of Physics, Albert-Einstein-Str. 23, 18059 Rostock, Germany*

[2] *micromod Partikeltechnologie GmbH, Friedrich-Barnewitz-Str. 4, 18119 Rostock, Germany*

6.1 Introduction

Standard cancer therapies are based on surgery, chemotherapy, irradiation or combinations of these methods. Among the multiple attempts of alternative therapy concepts hyperthermia plays an important role [1]. Besides the whole body hyperthermia in which the body temperature is systematically raised to 41.8°C, there are different types of local hyperthermia using microwave radiation, capacitive or inductive coupling of radiofrequency fields, implanted electrodes, ultrasounds or lasers [1]. In local hyperthermia the temperature increase compared to the standard temperature of human body is considered to be therapeutically useful over a relatively broad temperature range with different mechanisms of cell damages by increasing temperature. Two different types of local hyperthermia will be further addressed – treatments of temperature of 42°C to 45°C for up to few hours, which is actually denoted as hyperthermia and mainly requires a combination with a toxic agent for a reliable damage of the cancer cells, and thermoablation which aims for the thermal killing of cancer cells applying temperatures of at least 50°C in the tumor region for several minutes [1, 2]. Using magnetic nanoparticles (MNPs) for local hyperthermia including actual hyperthermia and thermoablation, particles are dispersed into the target tissue and an external alternating magnetic field with a certain field strength and frequency is applied. This leads to heating of the particles via Neel loss, Brown loss, hysteresis or frictional losses [1, 3].

The heating efficiency, the specific power loss (SPL), of the particles depends on the magnitude of the magnetic fields for a given frequency as well as the properties of the MNPs themselves [1, 4]. The most influential factors are saturation magnetization, anisotropy, relaxation time, particle concentration, Brownian motion and inter-particle interactions as well as particle size, core size, size distribution, particle shape and crystallinity [1, 4, 5].

The specific power loss SPL is related to the loss power density P, which for example is for superparamagnetic nanoparticles in the linear response theory connected to the imaginary part of the susceptibility χ'', the magnetic field H and the frequency f by [1]:

$$P(f, H) = \mu_0 \pi \chi''(f) H^2 f .$$

Therefore, it is a function of the external field and the frequency, nevertheless the increase of f and H is limited due to technical but also medical limitation. Due to an alternating magnetic field also eddy currents are induced in the body of the patient leading to an unwanted heating of cancerous as well as healthy tissue reducing the selectivity [1]. A limiting criterion for the product of magnetic field and frequency was determined for current loop with a diameter of 30 cm to be

$4.85 \cdot 10^8$ $Am^{-1}s^{-1}$ [1, 6]. Depending on the body region being exposed to the alternating magnetic field and the seriousness of the cancer this product may be exceeded.

The common measure of the SPL is the specific absorption rate (SAR) and is associated by the unit mass of magnetic material involved [5]:

$$SAR = \frac{m_{sample}}{m_{iron\ oxide}} \cdot C_m \cdot \frac{\Delta T}{\Delta t}$$

Where C_m is the specific heat capacity of the sample, m_{sample} and $m_{iron\ oxide}$ are the masses of the ferrofluid and the iron oxide, respectively, and ΔT is the temperature increase and Δt the time interval.

This overview will consider MNPs from **micromod** that were demonstrated to be interesting tools for hyperthermia applications. Especially MNPs of the product types nanomag®-D-spio, nanomag®-D and Bionized NanoFerrite (BNF) with nominal hydrodynamic diameters of 20 nm to 250 nm were investigated in various hyperthermia studies. These particles provide high heating rates and suitable surface modifications to improve colloidal stability, prevent aggregation of nanoparticles, ensure non-toxic status in physiological conditions and allow the introduction of functional groups for binding of target-specific biomolecules for hyperthermia applications. Targeted applications of MNPs for hyperthermia are summarized in chapter 8.

6.2 Characterization of MNPs for hyperthermia application

Bordelon et al. reported that the amplitude-dependent heating properties (4 kA/m to 94 kA/m) of Bionized NanoFerrite (BNF) nanoparticles and nanomag®-D-spio both with a hydrodynamic diameter of 100nm, and Feridex® particles with a hydrodynamic diameter in the range of 120 nm to 180 nm show qualitatively different behavior [4]. For the realization of the studies a calorimeter coil was developed to generate fields up to 100 kA/m at a frequency of 150 kHz. The considerable changes in the amplitude-dependent heating suggests that the particles have significantly different magneto-structural differences beside their similar size regimes and their chemical composition [4]. Strong interactions between the particles exist and are especially pronounced for the BNF particles, contributing to the heating of the particles in an external magnetic field [4].

Two types of BNF particles were produced with a different thickness of the dextran shell to investigate the influence of the shell thickness on the heating properties. Both kinds of BNF particles, once with a single dextran and the second with a double dextran layer, showed similar saturation magnetization, anisotropy and volume of the particles but significantly different SAR values of 150 W/g(Fe) and 1075 w/g(Fe), respectively, measured at 86 kA/m and 150 kHz [7]. Due to the double dextran coating of the particles the interaction radius of the particles was increased by a factor of approximately 3 [7].

Furthermore, the specific absorption rate of BNF particles with different hydrodynamic diameters of 30 nm, 60 nm and 90 nm was studied in dependence on the amplitude of the alternating magnetic field (AMF) for a frequency of 153 kHz (Fig. 1). With an increasing particle size a direct increase of the SAR can be observed as well as an increasing SAR for increasing amplitudes [8].

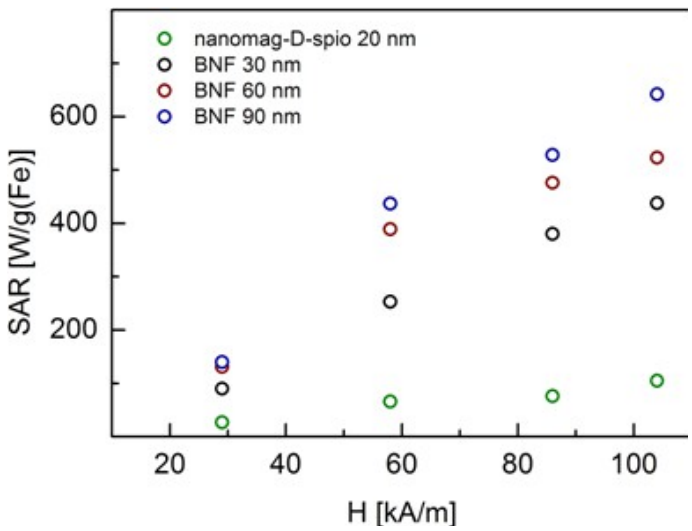

Figure 1. SAR of the BNF 30 nm, 60 nm, 90 nm and nanomag®-D-spio particles in dependence of the amplitude of the magnetic field for a frequency of 153 kHz (compare [8]).

6.3 Basic studies on advantages and limitations of hyperthermia with MNPs

6.3.1 Optimization of magnetic field strength and duration of hyperthermia treatment

It was expected that inter-particle interactions may affect the heating of MNPs in an AMF in two ways: the dipolar interaction will be significantly stronger for couple particles in an oscillating magnetic field and thereby amplifying the heating and due to the small interaction radius compared to the particle size particles group closer together enhancing the local heat output [7, 9]. *In vivo* mouse therapy was performed in an AMF inductor with twelve female mice (C3H/HeJ) bearing MTG-B murine breast tumors with a volume of 180 ± 40 mm^3 [9]. The particle suspension was directly injected into the central region of the tumor after the mice were anaesthetized and treated with different external magnetic fields. Each mouse received a normalized dose of particles per tumor volume (4.98±0.03 mg(Fe)/cm^3) [9]. The therapy was adjusted by varying the amplitude of the magnetic field and the duration of the therapy using a fixed frequency of 150 kHz. The therapy began when the tumor reached a temperature of 40.5 °C and terminated after 15 min, or when the rectal temperature of the mouse reached 41.5 °C or the tumor temperature 55 °C [9]. At higher field amplitudes the heat dose or SAR created a rapid heating leading to shorter treatment time [9]. When the magnetic field amplitude was 55.7 kA/m or higher the SAR increased drastically and produced substantial intra-tumor heating with the used nanoparticles, but also non-specific heat deposition by eddy currents was increased [9]. Nevertheless, a greater

therapeutic response was achieved using higher magnetic fields with a shorter duration of the treatment. Experimental evidence demonstrated that for interacting BNF nanoparticles, determined by their spacing and anisotropy, the resulting collective behavior in the kilohertz frequency regime generates significant heat, leading to nearly complete regression of aggressive mammary tumors in mice [9].

6.3.2 Relation between cancer cell association with MNPs and tumor cell cytotoxicity

The physical association of cancer cells with MNPs was studied to determine the nanoparticle-induced cytotoxicity [10]. The time dependent cellular uptake of intratumorally administered iron oxide nanoparticles in a murine breast adenocarcinoma cell line (MTG-B) was studied *in vivo*. Tumors with averaging volumes of 115 mm^3 were injected with 100 nm BNF-Dextran particles. The tumors were then excised and fixed for TEM at time 0.1–120 h after injection. Intracellular uptake was 5.0, 48.8 and 91.1% uptake at one, 2 and 4 h post-injection, respectively, suggesting two time domains for intratumorally delivered MNP hyperthermia. Based on the observations of Giustini et al., there does not appear to be a specific anatomic location of the nanoparticles within the cells. Once tumor cells have aggregated the nanoparticles intracellularly, more heat will be deposited into the tumor upon AMF activation with the same field strength and frequency, resulting in greater tumor cytotoxicity [10].

6.3.3 BNF particles as tools for numerical modeling of local heat transfer boundary conditions

Pearce et al. developed a numerical model based on finite element method that reveals the extent and dominance of local heat transfer boundary conditions and provides a new approach that may simplify the numerical problem sufficiently to make ordinary computer machinery capable of generating useful predictions [11]. Two numerical model series were executed assuming uniform nanoparticle heating in a magnetic field with uniformly dispersed individual nanoparticles and with clusters of MNPs of varying size in single- and multiple-cell sized model spaces. Experimental studies provided calibration and guidance for the numerical model studies [11]. A mouse flank tumor was injected with 100 nm BNF-Starch particles and heated for 24 min in a magnetic field with 48 kA/m peak to peak. The surface temperature was monitored reaching 42°C after 17 min of the treatment. Numerical results showed the importance of nanoparticles clustering to achieve adequate heating [11]. The volume powder generation to achieve therapeutic values decreases dramatically when the distance between unheated isothermal surfaces increases. It was shown that local heat transfer is the dominant mechanism [11] supporting the suggestion that the minimal treatable tumor size is likely about 2 mm in radius [12]. It was pointed out that to achieve tissue heating with nanoparticles and nanoparticle constructions the nanoparticle-nanoparticle association, the total iron dose, the volumetric powder density and the tissue geometry have to be matched [11].

6.3.4 Determination of the minimum tumor size for nanoparticle-mediated hyperthermia

Hedayati et al. studied the influence of cell cluster size on intracellular nanoparticle hyperthermia. Therefore DU145 cells were cultured in flasks in the presence of poly-D-lysine coated 100 nm BNF–Starch nanoparticles [13]. Afterwards cell pellets were formed and exposed to an AMF with amplitudes in the regime of 50 Oe to 1200 Oe for *in-situ* measuring the temperature of the pellets. The measured surface temperatures were consistent with those predicted by a heat diffusion model ignoring intercellular thermal barriers [13]. After heat treatment the cells were plated and the fractional survival was determined by a clonogenic assay [13]. It was shown that for a given intracellular nanoparticle concentration, a critical minimum number of cells is required for cytotoxic hyperthermia. Above this threshold, the cytotoxicity increases with raising cell number. It was suggested that the minimum tumor volume threshold is 1 mm^3 below which nanoparticle-mediated heating is unlikely to be effective as the only cytotoxic agent [13].

6.3.5 Protection of healthy tissue at hyperthermia treatment

To assess the potential for injuries of normal tissue by hyperthermia treatment in mice, twenty three male nude mice received intravenous injections of 100 nm nanomag®-D-spio particles on three days and were exposed to an AMF on the sixth day. A day later, the blood, liver and spleen were harvested and analyzed [14]. Each mouse was treated for 30 min in an AMF with a frequency in the regime of 140–160 kHz with amplitudes of 0 kA/m, 24 kA/m and 60 kA/m. In this pilot study it was demonstrated, that MNPs producing only modest heat output can cause damage, and even death, when sequestered in sufficient concentrations. The superparamagnetic iron oxide dextran nanoparticles are deposited in liver and spleen, making these the sites of potential toxicity [14].

6.3.6 Image-guided hyperthermia therapy of liver cancer

In a feasibility study, Attaluri et al. sought to determine whether a formulation composed of MNP iron oxide multi-crystallite cores and ethiodised oil might provide sufficient heating using AMFs and image-guidance for transcatheter intra-arterial and intratumoral delivery in animal models [15]. The developed formulation, called BNF-lip, comprises 100 nm BNF-Starch particles emulsified with polysorbate 20 in ethiodised oil. *In vivo* thermal therapy capability was tested in two groups of male $Foxn1^{nu}$ mice bearing subcutaneous HepG2 xenograft tumors. Group I was used to screen conditions for group II. In group II, mice received one of BNF-lip, BNF alone, or PBS, followed by alternating magnetic field hyperthermia, with different durations (15 or 20 min) and amplitudes (0, 16, 20, or 24 kA/m). Furthermore, image-guided fluoroscopic intra-arterial injection of BNF-lip was tested in New Zealand white rabbits, bearing liver VX2 tumors. The tumors were histopathologically evaluated for distribution of BNF-lip. The BNF-lip formulation produced maximum tumor temperatures with AMF amplitudes larger than 20 kA/m (Fig. 2) and showed positive X-ray visibility and substantial shortening of T1 and T2 relaxation time, with sustained

intratumoral retention up to 7 days post-injection [15]. Intratumoral BNF-lip distribution correlated well with CT imaging of intratumoral BNF-lip distribution. The BNF-lip formulation has favorable thermal and dual imaging capabilities for image-guided thermal therapy of liver cancer.

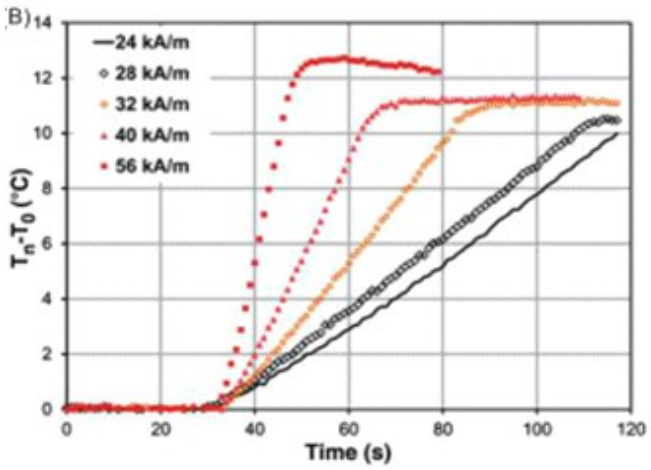

Figure 2. Specific heating rate measurements of BNF-lip formulation with varying amplitude at 155 kHz.

6.3.7 Comparison of MNP assisted hyperthermia and microwave hyperthermia

Comparing the effects of hyperthermia with MNPs to microwave hyperthermia treatment thermal doses equivalent to 60 min at 43°C were delivered to syngeneic mouse mammary adenocarcinoma flank tumors using both heating methods [16]. The MNPs used in the study were 100 nm BNF-Starch. After delivery of the particles the mouse tumor was exposed to an alternating magnetic field with a frequency of 165 kHz and a magnetic field strength of 35.8 kA/m obtaining a SAR of 151 W/g(Fe). The microwaves used in the study had a frequency of 915 MHz and were applied with a surface applicator. The time required for the tumor to reach three times the treatment volume was used as the endpoint of the primary study. The locally delivered particles resulted in a modest improvement in treatment efficacy as compared to microwave hyperthermia considering the same thermal dose [16]. Additionally, the tumors treated with MNP hyperthermia also demonstrated a reduction of the peritumoral normal tissue damage suggesting an improvement of the therapeutic ratio for locally delivered tumor hyperthermia [16].

6.4 Non-temperature induced effects of magnetized MNPs in AMF in cancer cells

The damaging effects of MNPs on magnetically labelled cancer cells when subjected to oscillating gradients in a strong external magnetic field were studied. Human breast cancer cells were labeled with plain 80 nm BNF-Starch particles, placed in the high magnetic field, and subjected to oscillating gradients generated by an imaging gradient system of a 9.4T preclinical MRI system. Changes in cell morphology and a decrease in cell viability were detected in cells treated with oscillating gradients. An approximately 26.6% reduction in cell viability was detected in magnetically labeled cells subjected to the combined effect of a static magnetic field

and oscillating gradients. No reduction in cell viability was observed in unlabeled cells subjected to gradients, or in MNP-labeled cells in the static magnetic field. As no increase in local temperature was observed, the cell damage was not a result of hyperthermia. Hapuarachchige et al. consider the coherent motion of internalized and aggregated nanoparticles that produce mechanical moments as a potential mechanism of cell destruction. This strategy provides a new way to eradicate a specific population of MNP-labeled cells, potentially with MRI guidance using standard MRI equipment, with minimal side effects for the host [17].

6.5 Hyperthermia for immune-related therapies

In vitro experiments using magnetically-loaded dendritic cells as vectors for thermotherapy have shown the potential of this 'Trojan horse' strategy for immune-related therapies. Therefore, the effects of alternating magnetic fields on the death rate of dendritic cells containing MNPs were investigated [18, 19]. Human-monocyte-derived dendritic cells were co-incubated with functionalized 250 nm nanomag®-D particles [18]. The cells were exposed to external alternating magnetic fields using field strengths of 3.2, 6.4, 9.5 and 12.7 kA/m at a constant frequency of 260 kHz for 5, 10 and 15 min. The viability of the dendritic cells could be controlled by the choice of the field strength and exposure time as well as the amount of particles loaded. About 20% of cells showed Annexin-negative/PI-positive staining after 5–10 min of exposure to the alternating magnetic field [18]. Necrotic-like populations were observed after exposure times of 10 min pointing out that locally relevant cell structures or metabolic processes can yield irreversible cell damage. Nevertheless, controlled cell death of dendritic cells containing MNPs was observed by adequate tuning of the parameters of the AMF and the concentration of the nanoparticles [18].

Staphylococcus aureus (*S. aureus*) has emerged as a leading cause of colonization and infection in various soft-tissue wounds including venous leg ulcers and diabetic foot ulcers resulting in the development of chronic non-healing wounds [20]. A novel antimicrobial magnetic thermotherapy was proposed in which an AMF is used to rapidly heat magnetic particle conjugated *S. aureus.* Therefore streptavidin coated 100 nm nanomag®-D-spio particles were conjugated to biotinylated anti-proteinA mAb and locally injected into the infected wound. Heating could facilitate efficient and rapid inactivation of bacterial cells and biofilms without further compromising fragile patients or exacerbating drug resistance [20]. The antimicrobial efficacy of this platform was evaluated in the treatment of both an *in vitro* culture model of *S. aureus* biofilm and a mouse model (EGFP-lys mice) of cutaneous *S. aureus* infection. In the systematic study, the bacteria were exposed to the nanomag®-D-spio particles in varying concentrations and exposed to an AMF with a field strength of 18 kA/m, 31 kA/m and 40 kA/m using a frequency of 2.1 MHz for 3 min. A 99.9% reduction in *S. aureus* bioluminescence was achieved at a dose of 150 µg nanoparticles at 40 kA/m and 99% at 200 µg using 31 kA/m demonstrating that an antibody-targeted MNP bound to *S. aureus* was effective at thermally inactivating *S. aureus* [20].

6.6 Summary

The development of MNPs for hyperthermia applications significantly increased over the last decades. Particles from **micromod** were studied in a broad variety of hyperthermia studies with different focusses from the basic to the applied research. An overview on the nanoparticles that were described in this review is given together with the core size, the hydrodynamic particle diameter and the parameters of the AMFs for the hyperthermia treatment in Table 1. The outstanding magnetic properties and the high diversity of surface functionalizations allow the use of BNF and nanomag®-D particles as interesting tools in hyperthermia applications. A short review on targeting of MNPs for hyperthermia applications is given in chapter 8.

Tab.1: Overview of the MNPs used for heating experiments with specific SAR values for a given field strength and frequency.

Particle name	Hydrodynamic diameter [nm]	Surface	SAR [W/g(Fe)]	H [kA/m]	f [kHz]	Reference
BNF	30	dextran	90 253 380 438	29 58 86 104	153 153 153 153	[8]
BNF	60	dextran	131 389 476 523	29 58 86 104	153 153 153 153	[8]
BNF	90	dextran	140 437 528 642	29 58 86 104	153 153 153 153	[8]
BNF	108 110	starch	11 78 278 537 151	12 24 40 94 35.8	150 150 150 150 165	[4, 5] [16]
BNF	100	dextran	250	35.8	150	[21]
nanomag®-D-spio	86	dextran	44 91 116 162	12 24 40 94	150 150 150 150	[4, 5]
nanomag®-D-spio	20	dextran	27 66 76 105	29 58 86 104	153 153 153 153	[8, 22]
nanomag®-D-spio	100	dextran/ streptavidin	900	31	2100	[20]

References

[1] Hergt, R., et al., *Magnetic particle hyperthermia: nanoparticle magnetism and materials development for cancer therapy.* Journal of Physics: Condensed Matter, 2006. **18**(38): p. S2919.

[2] Dennis, C., et al., *The influence of magnetic and physiological behaviour on the effectiveness of iron oxide nanoparticles for hyperthermia.* Journal of Physics D: Applied Physics, 2008. **41**(13): p. 134020.

[3] Colombo, M., et al., *Biological applications of magnetic nanoparticles.* Chem Soc Rev, 2012. **41**(11): p. 4306-34.

[4] Bordelon, D.E., et al., *Magnetic nanoparticle heating efficiency reveals magneto-structural differences when characterized with wide ranging and high amplitude alternating magnetic fields.* Journal of Applied Physics, 2011. **109**(12): p. 124904.

[5] Grüttner, C., et al., *Synthesis and functionalisation of magnetic nanoparticles for hyperthermia applications.* International Journal of Hyperthermia, 2013. **29**(8): p. 777-789.

[6] Brezovich, I.A., *Low frequency hyperthermia: capacitive and ferromagnetic thermoseed methods.* Medical physics monograph, 1988. **16**: p. 82-111.

[7] Dennis, C., et al., *The influence of collective behavior on the magnetic and heating properties of iron oxide nanoparticles.* Journal of Applied Physics, 2008. **103**(7): p. 07A319.

[8] Grüttner, C., et al., *Synthesis and antibody conjugation of magnetic nanoparticles with improved specific power absorption rates for alternating magnetic field cancer therapy.* J. Magn. Magn. Mat., 2007. **311**(1): p. 181-186.

[9] Dennis, C., et al., *Nearly complete regression of tumors via collective behavior of magnetic nanoparticles in hyperthermia.* Nanotechnology, 2009. **20**(39): p. 395103.

[10] Giustini, A., R. Ivkov, and P. Hoopes, *Magnetic nanoparticle biodistribution following intratumoral administration.* Nanotechnology, 2011. **22**(34): p. 345101.

[11] Pearce, J., et al., *Magnetic Heating of Nanoparticles: The Importance of Particle Clustering to Achieve Therapeutic Temperatures.* Journal of Nanotechnology in Engineering and Medicine, 2013. **4**(1): p. 0110071-01100714.

[12] Etheridge, M. and J. Bischof, *Optimizing magnetic nanoparticle based thermal therapies within the physical limits of heating.* Annals of biomedical engineering, 2013. **41**(1): p. 78-88.

[13] Hedayati, M., et al., *The effect of cell-cluster size on intracellular nanoparticle-mediated hyperthermia: is it possible to treat microscopic tumors.* Nanomedicine, 2012. **8**(1): p. 29-41.

[14] Kut, C., et al., *Preliminary study of injury from heating systemically delivered, nontargeted dextran-superparamagnetic iron oxide nanoparticles in mice.* Nanomedicine, 2012. **7**: p. 1697-1711.

[15] Attaluri, A., et al., *Image-guided thermal therapy with a dual-contrast magnetic nanoparticle formulation: A feasibility study.* International Journal of Hyperthermia, 2016. **32**(5): p. 543-557.

[16] Petryk, A.A., et al., *Comparison of magnetic nanoparticle and microwave hyperthermia cancer treatment methodology and treatment effect in a rodent breast cancer model.* International Journal of Hyperthermia, 2013. **29**(8): p. 819-827.

[17] Hapuarachchige, S., et al., *Non-Temperature Induced Effects of Magnetized Iron Oxide Nanoparticles in Alternating Magnetic Field in Cancer Cells.* PLoS ONE, 2016. **11**(5): p. e0156294.

[18] Asin, L., et al., *Controlled cell death by magnetic hyperthermia: effects of exposure time, field amplitude, and nanoparticle concentration.* Pharm. Res., 2012. **29**: p. 1319-1327.

[19] Asin Pardo, L., *Biomedical applications of magnetic nanoparticles: magnetic hyperthermia in dendritic cells and magnetofection in brain cells.* PhD thesis, University of Zaragoza, Spain, 2012.

[20] Kim, M.-H., et al., *Magnetic nanoparticle targeted hyperthermia of cutaneous staphylococcus aureus infection.* Ann. Biomed. Eng., 2013. **41**(3): p. 598-609.

[21] Zhang, J., et al., *Herceptin-directed nanoparticles activated by an alternating magnetic field selectively kill HER-2 positive human breast cancer cells in vitro via hyperthermia.* Int. J. Hyperthermia, 2011. **27**(7): p. 682-697.

[22] DeNardo, S.J., et al., *Development of tumor targeting bioprobes (111In-chimeric L6 monoclonal antibody nanoparticles) for alternating magnetic field cancer therapy.* Clinical Cancer Research, 2005. **11**(19): p. 7087s-7092s.

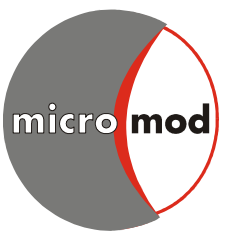

Editor:
micromod Partikeltechnologie GmbH

Registergericht: Amtsgericht Rostock HRB 5837
Steuernummer: 4079/114/03352
Ust-Id Nr. (Vat No.): DE167349493

Compilation date - May the 10th, 2017
micromod Partikeltechnologie GmbH

www.micromod.de